

ARTICLE OPEN

GABA_A receptor availability in clinical high-risk and first-episode psychosis: a [¹¹C]Ro15-4513 positron emission tomography study

Paulina B. Lukow^{1,2}✉, Julia J. Schubert³, Mario Severino⁴, Samuel R. Knight⁵, Amanda Kiemes², Nicholas R. Livingston⁶, James Davies⁵, Andrea de Micheli⁶, Thomas J. Spencer⁶, Paolo Fusar-Poli^{6,7,8,9}, Beate Haeghe¹⁰, Natasha Vorontsova⁶, Jacek Donocik¹¹, Eugenii A. Rabiner⁵, Anthony A. Grace¹², Steven C. Williams¹³, Philip McGuire^{13,14}, Mattia Veronese¹⁵, Federico E. Turkheimer¹⁵ and Gemma Modinos^{2,15}

© The Author(s) 2025

Disrupted gamma-aminobutyric acid (GABA) neurotransmission may contribute to the pathophysiology of schizophrenia. Reductions in hippocampal GABAergic neurons have been found in schizophrenia, and increased hippocampal perfusion has been described in schizophrenia and in people at clinical high-risk for psychosis (CHRp). We have also found decreases in hippocampal GABA_A receptors containing the α5 subunit (GABA_ARα5) in a well-validated neurodevelopmental rat model of relevance for schizophrenia. Positive allosteric modulation of these receptors in the hippocampus using a specific compound was shown to reverse the behavioural and neurophysiological phenotypes of this model. However, whether GABA_ARα5 availability is dysregulated in the psychosis spectrum at the regional or network levels is unknown. We addressed this issue by using [¹¹C]Ro15-4513 and positron emission tomography (PET) in 22 individuals at CHRp, 10 people with a first-episode psychosis (FEP) and 23 healthy controls (HC). We quantified GABA_ARα5 availability in the hippocampus and across the brain, and employed a perturbation covariance method to assess individual molecular covariance deviations in CHRp and FEP groups compared to the HC group. Hippocampal GABA_ARα5 availability was not significantly different between groups ($F(2,50) = 0.25$, $p = 0.78$). However, network analysis identified significant deviations in GABA_ARα5 covariance between groups, both across all regions (all $p < 0.001$, pairwise Cohen's $d = 0.07$ – 0.5) and relative to the hippocampus (all $p < 0.001$, pairwise Cohen's $d = 0.01$ – 0.67). These findings suggest that individuals at clinical high-risk for psychosis and people with early psychosis may show alterations to the brain-wide organisation of the GABA_ARα5 system, rather than changes at a regional level.

Molecular Psychiatry (2026) 31:987–996; <https://doi.org/10.1038/s41380-025-03204-9>

INTRODUCTION

There is growing interest in the role of gamma-aminobutyric acid (GABA)ergic dysfunction in psychosis. The loss of GABAergic interneurons in the hippocampus has been found in post-mortem studies of people with schizophrenia [1–3] and increased hippocampal perfusion has been found in individuals with schizophrenia in vivo [4, 5]. Similar findings have been reported in people at clinical high-risk for psychosis (CHRp) [6–8], who experience sub-threshold psychotic symptoms [9–11] and are at 25% risk of transition to frank psychosis [12]. Despite extensive research, the biological mechanisms underlying different degrees of psychosis symptoms remain largely unknown [6–8].

A mechanistic investigation of hippocampal hyperactivity in psychosis development has been provided by studies employing the methylazoxymethanol acetate (MAM) rodent model. This model involves administration of the mitotoxin MAM to pregnant rats on gestational day 17, which interferes with hippocampus development [13] and results in local hyperactivity [14]. Upon reaching adulthood, MAM rats present with a number of behaviours consistent with a psychosis-relevant phenotype: elevated response to amphetamine administration, a decrease in social interaction, reduced executive function, a lower startle threshold and a deficit in attenuating startle response to repetitive stimuli [13]. Additionally, they exhibit elevated dopamine release into the striatum [14, 15], a phenomenon found robustly in

¹Institute of Cognitive Neuroscience, University College London, Alexandra House, 17-19 Queen Square, London WC1N 3AZ, UK. ²Department of Psychological Medicine, Institute of Psychiatry, Psychology & Neuroscience, King's College London, 16 De Crespigny Park, London SE5 8AB, UK. ³Department of Neuroimaging, Institute of Psychiatry, Psychology & Neuroscience, King's College London, 16 De Crespigny Park, London SE5 8AB, UK. ⁴Department of Information Engineering, University of Padova, Via Giovanni Gradenigo, 6B, 35131 Padova, Italy. ⁵Invicro, Burlington Danes Building, Imperial College London, Hammersmith Hospital, Du Cane Road, London W12 0NN, UK. ⁶Department of Psychosis Studies, Institute of Psychiatry, Psychology & Neuroscience, King's College London, 16 De Crespigny Park, London SE5 8AB, UK. ⁷Department of Brain and Behavioral Sciences, University of Pavia, Pavia, Italy. ⁸Outreach and Support in South-London (OASIS) service, South London and Maudsley (SLaM) NHS Foundation Trust, London, UK. ⁹Department of Psychiatry and Psychotherapy, University Hospital, Ludwig-Maximilian-University (LMU), Munich, Germany. ¹⁰Southwark Team for Early Psychosis, South London and Maudsley NHS Foundation Trust, St Giles House, 1 St Giles Road, London SE5 7UD, UK. ¹¹Lewisham Early Intervention Service, South London and Maudsley NHS Foundation Trust, 59 Cordwell Road, Lewisham, London SE13 5QY, UK. ¹²Departments of Neuroscience, Psychiatry and Psychology, University of Pittsburgh, Pittsburgh, PA 15260, USA. ¹³Department of Psychiatry, University of Oxford, Warneford Hospital, Oxford OX3 7JX, UK. ¹⁴NIHR Oxford Health Biomedical Research Centre, Oxford OX3 7JX, UK. ¹⁵MRC Centre for Neurodevelopmental Disorders, King's College London, London, UK. ✉email: p.lukow@ucl.ac.uk

Received: 25 February 2025 Revised: 9 June 2025 Accepted: 27 August 2025

Published online: 6 September 2025

psychosis and schizophrenia [16] and two independent samples of CHRp individuals [17]. The hippocampus regulates striatal function through direct projections [18] and indirectly through ventral tegmental area (VTA) disinhibition [19, 20]. Interestingly, MAM rats also show alterations to the GABAergic system in the hippocampus, providing insight into the molecular mechanisms linking hippocampal dysfunction, striatal hyperdopaminergia and psychosis.

GABAergic interneuron loss has been found in the hippocampus of adult MAM rats [21]. This finding is analogous to the generally decreased nonpyramidal cell numbers [1], and a reduction in specific cell-type densities [2] and numbers [3] in the hippocampus in schizophrenia. Interestingly, peripubertal amplification of GABAergic function in MAM rats with the benzodiazepine diazepam was shown to prevent MAM phenotype emergence and GABAergic inhibitory interneuron loss in the hippocampus [21, 22]. However, benzodiazepines show affinity for several GABA_A receptors expressed across the brain [22]. In this context, GABA_A receptors containing the $\alpha 5$ subunit (GABA_AR $\alpha 5$) are an attractive target due to being predominantly expressed in the hippocampus [23]. Direct infusion into the hippocampus of a selective GABA_AR $\alpha 5$ positive allosteric modulator in adult MAM rats was shown to normalise the dopaminergic output from the VTA into the striatum, and the exaggerated hyperlocomotor response to amphetamine [24]. Furthermore, genetic $\alpha 5$ subunit deletion in mice was found to produce a phenotype similar to that of adult MAM rats [24]. Moreover, our recent *ex vivo* autoradiography study with [³H]Ro15-4513 in MAM rats showed lower density of GABA_AR $\alpha 5$ across the hippocampus [25]. Altogether, this suggests a potential role of GABA_AR $\alpha 5$ alterations in psychosis, making them a possible novel therapeutic target for this disorder.

GABA_AR $\alpha 5$ represent about 30% of all GABA_ARs in the hippocampus, but only 7–8% of them across the brain [26]. They are predominantly extrasynaptic and show high affinity for GABA, which facilitates tonic inhibition of neural firing in response to ambient neurotransmitter levels [27, 28]. A reduction in GABA_AR $\alpha 5$ -mediated tonic inhibition in the hippocampus could lead to an increase in local pyramidal neuron firing rate, resulting in hyperactivity. However, evidence supporting such hypothesis from human studies remains limited. Very few post-mortem studies assessed hippocampal GABAergic receptor availability in schizophrenia, and neither used a label selective for receptors containing a specific subunit [29–31]. Post-mortem studies may be affected by long illness duration, medication exposure and death, further limiting interpretability. Here, positron emission tomography (PET) can be used to measure receptor availability in the human brain *in vivo* in different populations from the psychosis spectrum.

The two most common GABA_AR PET radiotracers are radiolabelled flumazenil and Ro15-4513 [32]. While the former has similar affinity for a number of GABA_ARs [33], the latter shows high specificity for GABA_AR $\alpha 5$, to which it binds allosterically [34]. To date, GABA PET studies in individuals at clinical high-risk for psychosis and people with early psychosis using either radiotracer have been inconclusive. Experiments in schizophrenia using radiolabelled flumazenil found inconsistent results, with only one [35] of the two [35, 36] available studies reporting increased binding in the hippocampus of antipsychotic-naïve schizophrenia patients. Studies employing [¹¹C]Ro15-4513 found unchanged [37] or decreased [38] binding in the hippocampus in schizophrenia. The only GABA PET study in the CHRp population found no changes in [¹⁸F]flumazenil binding in the hippocampus [39]. However, several of these studies employed quantification relying on comparison to a reference region, an approach which may have not been sensitive enough for the study of GABAergic function, as no region in the brain is devoid of GABA_ARs [40]. Therefore, an investigation of GABA_AR $\alpha 5$ availability in individuals at CHRp and with early psychosis using full tracer kinetic quantification is warranted.

While evidence suggests that neurotransmission may be altered regionally in psychosis, it has also been posited that the symptomatology may emerge from network-level dysfunction [41]. A novel method that allows addressing this question using neuroimaging data is the perturbation network covariance approach [42, 43]. This is a statistical framework used to construct single-participant-specific networks that reveal abnormalities in e.g., individual molecular covariance patterns relative to a reference sample (e.g., healthy controls) [44]. These patterns are then averaged across all participants to investigate group perturbations across the network. We sought to complement standard group comparisons by additionally employing the kinetic modelling quantification parameters in this network-based approach, to comprehensively characterise brain-wide GABA_AR $\alpha 5$ organisation in people at CHRp or with an FEP.

The present study aimed to use [¹¹C]Ro15-4513 PET with full tracer kinetic quantification methods in CHRp individuals and people with a first-episode of psychosis (FEP) to examine regional binding; and, to conduct a brain-wide perturbation covariance analysis to evaluate individual molecular covariance deviations from the reference healthy controls. We hypothesised that there would be a reduction in [¹¹C]Ro15-4513 binding in the hippocampus of individuals at CHRp and people with an FEP; and that both CHRp and FEP individuals would exhibit significant molecular inter-regional deviations relative to the healthy control group.

METHODS

Participants

Twenty-four individuals at CHRp and ten with an FEP were recruited from the South London and Maudsley NHS Trust [45]. Twenty-four healthy controls (HC) were additionally recruited through public advertisement from the same geographical area. All participants had capacity for consent, were between 18–40 years old, had no neurological or major medical conditions (e.g., aneurysm, severe asthma), had an IQ ≥ 70 estimated by the Wechsler Adult Intelligence Scale (WAIS-III) [46], presented adequate collateral circulation in the hand, had no history of clotting or renal abnormality, were not currently exposed to any drug with a GABAergic or glutamatergic mechanism of action, had no contraindication to MRI, did not donate >500 ml of blood within 60 days prior to scanning, did not have radiation exposure exceeding >10 mSv in preceding 12 months, had no past or present history of substance abuse, and were not pregnant or breastfeeding. Healthy blood clotting was ascertained with the international normalised ratio test and the activated partial thromboplastin time test. CHRp state was defined by presence of current attenuated psychosis symptoms, according to the Comprehensive Assessment for At-Risk Mental States (CAARMS) [47]; participants with additional brief limited intermittent psychotic symptoms (BLIPS) [48–51] or family history of psychotic disorder were included. Only CHRp participants without any previous or current history of psychosis (excluding BLIPS) or antipsychotic exposure were included. CHRp participants with current or past antidepressant exposure were included. Additional inclusion criteria for FEP participants included an ICD-10 diagnosis of psychotic disorder (F20-F29 and F31) [52], at least one rating of moderate severity on the positive subscale of the Positive and Negative Syndrome Scale (PANSS) [53] and ‘first treatment contact’, i.e., receiving support from an Early Intervention mental health service for a period of less than two years since first admission. Participants with an FEP were included if they never received any antipsychotic medication, were not currently taking antipsychotic medication, or were on a stable dose of any antipsychotic other than clozapine and were not treatment refractory. Additional inclusion criteria for HC participants were no self-reported history of Axis I mental health disorder and no personal or familial history of psychosis. The study obtained ethical approval from the London/Surrey Research Ethics Committee (17/LO/1130). All participants provided written informed consent before participation, in accordance with The Declaration of Helsinki [54].

PET acquisition

Scanning was performed on a SignaTM PET-MR General Electric (3T) scanner using the MP26 software (01 and 02) at Invicro, an imaging centre located in London, UK. The radiotracer was administered through the dominant

antecubital fossa vein in a single bolus injection, administered at the beginning of the scanning session. Arterial blood sampling was performed from the radial artery in the non-dominant wrist for the production of a metabolite-corrected plasma input function. Continuous blood sampling was performed during the first 15 min of the scan, followed by up to 13 discrete samples (maximum 195 ml in total, including samples required for arterial line clearing). The mean \pm SD amount of radiation administered was 283.25 MBq \pm 72.79 (range: 124.13–404.75 MBq). PET acquisition was performed in 3D list mode for 70 min and binned in the following frames: 15s \times 10, 60s \times 3, 120s \times 5, 300s \times 11. Attenuation correction was performed with a ZTE sequence (voxel size: 2.4 \times 2.4 \times 2.4 mm³, field of view = 26.4, 116 slices, TR = 400 ms, TE = 0.016 ms, flip angle = 0.8°). A T1-weighted IR-FSPGR sequence was used for PET image co-registration (voxel size: 1 \times 1 \times 1 mm³, field of view = 25.6, 200 slices, TR = 6.992 ms, TE = 2.996 ms, TI = 400 ms, flip angle = 11°). Image reconstruction was done by ordered subset expectation maximization reconstruction with point spread function recovery and time-of-flight activated. A power calculation using G*Power on [¹¹C]Ro15-4513 PET data from a previous study [55] indicated that 20 participants per group were required to detect a significant change in binding with a power of 0.8 (alpha = 0.05, two-tailed).

Demographic and clinical data analysis

Clinical and demographic information about the study participants was collected at the assessment visit. Clinical information about the study sample included psychosis symptom severity (assessed with CAARMS in CHRp and HC, and with PANSS in FEP), anxiety and depression symptom severity (Hamilton Anxiety [56] and Depression [57] Rating Scales), current functioning (Global Functioning: Social and Role Scales [58]) and current neuroleptic medication. Demographic information included age, sex, ethnicity and self-reported substance use (including recency and frequency for caffeine, tobacco and alcohol, and current use for cannabis). There were no group differences in caffeine, tobacco, alcohol or cannabis use (Supplementary Methods and Results: Effects of recent substance use on regional and brain-wide [¹¹C]Ro15-4513 binding). Chlorpromazine equivalent doses of antipsychotic medication for people with an FEP on a stable dose were calculated using the *chlorpromazineR* package (<https://docs.ropensci.org/chlorpromazineR/>) in R 4.2.1 using the previously published conversion method [59–63].

Analysis of clinical and demographic data was performed in R 4.2.1. χ^2 test was used to analyse differences in sex between groups with the *chisq.test()* function. One-way ANOVA with the *anova.test()* function from the *rstatix* package (<https://CRAN.R-project.org/package=rstatix>) was used to compare differences between groups in other demographic and clinical variables. Post-hoc pairwise t-tests were used to determine differences between groups with the *pairwise_t.test()* function from the *rstatix* package, with the Holm multiple comparison correction method [64]. Results in all analyses were considered significant at $p < 0.05$. Missing data were omitted from analysis.

PET data quantification and quality checks

PET images were pre-processed with MIAKAT 4.3.24 in MATLAB R2017a. For each participant, an isotropic, skull-stripped IR-FSPGR structural image linearly transformed to the MNI template [65] was co-registered to an isotropic, motion-corrected integral image created from the PET time series. The CIC v2.0 neuroanatomical atlas [66] was non-linearly transformed to the participant's structural image and used to define the following regions of interest (ROIs): whole-brain, whole-brain grey matter, cortex, subcortical regions, cerebellum, brain stem, occipital lobe, insular cortex, temporal lobe, frontal lobe, cingulate cortex, parietal lobe, basal ganglia, thalamus, parahippocampal gyrus, amygdala, hippocampus, anterior cingulate cortex, globus pallidus, striatum, caudate, nucleus accumbens and putamen. Time-activity curves were extracted for each region of interest individually from the dynamic PET acquisition using the CIC v2.0 atlas [66] and then input into a two-tissue compartmental model using the regional brain tissue and the blood as the two compartments. The outcome measure from the two-tissue compartmental (2TCM) model was the total volume of distribution (V_T), in agreement with Horder et al. [67]. This approach was chosen instead of a single reference tissue model (SRTM) and the associated outcome measures BP_p or BP_{ND} due to SRTM's lower reliability (2TCM: ICC > 0.82, SRTM: ICC = 0.35–0.8 [55, 68]) and reliance on several assumptions, the violation of which can lead to biased estimates [69]. Furthermore, no region in the brain is devoid of GABA_ARs [40], precluding the use of an appropriate reference region. For instance, it has been shown that using the pons as a reference region may lead to the

underestimation of target binding despite its low [¹¹C]Ro15-4513 binding profile [68–70]. Pre-processing outputs (brain segmentation, motion correction, left-right image orientation consistency, motion correction, ROI fitting to individual brains, time-activity curves and parent plasma fraction plots for the hippocampus and whole-brain) were quality-checked visually for each participant. Poor quality data insufficient for quantification or with abnormal model fitting was excluded. Then, model parameters (V_T ; rate constant for transfer from arterial plasma to tissue, K_1 ; fractional volume of blood within a given region, V_b [71]) were assessed for the existence of outliers. A participant was considered for exclusion if at least 50% of their values across all ROIs exceeded the outlier detection threshold, which was at mean \pm 3 standard deviations for the whole study sample for a given ROI. No participants were excluded on this basis. If individual data points within included participant datasets were identified as outliers, they were considered for exclusion if the corresponding time-activity curve did not pass the quality check. No data points were excluded on this basis.

PET data analysis

Our primary outcome measure was hippocampal [¹¹C]Ro15-4513 binding. Between-group comparison of hippocampal [¹¹C]Ro15-4513 V_T values was performed including the three groups with a one-way ANOVA with age and sex as covariates of no interest. In a supplementary analysis to assess between-group differences in [¹¹C]Ro15-4513 binding across the brain, mixed ANOVAs were conducted including all regions tested, with age (mean-centred) and sex as covariates of no interest. All ANOVA models were fitted with the *anova.test()* function from the *rstatix* package. Effect sizes are reported in generalised eta squared (η^2) from the *anova.test()* output. The ANOVAs were repeated controlling for recent substance use (caffeine, tobacco, alcohol and cannabis). Post-hoc pairwise comparisons were performed with the *anova.test()* function from the *rstatix* package for each group pair. Results were considered significant if they passed Bonferroni correction for multiple comparisons. The Greenhouse-Geisser correction was applied to any interactions found which violated the assumption of sphericity (reported as p_{GG}). Correlations with symptoms were estimated using the *cor.test()* function from the *stats* package, omitting missing values. For the FEP group, the correlation analyses were repeated using partial correlations including antipsychotic dose (chlorpromazine equivalents) as a covariate of no interest (*pcor.test()* function, *ppcor* package). The sample size was sufficient for the assumption of normality [72]. The experiment was not repeated in our laboratory.

Covariance perturbation analysis

Covariance perturbation analysis [44] was performed to investigate group differences in brain-wide correlations in [¹¹C]Ro15-4513 binding. First, a reference network was constructed using HC data, by performing partial Pearson correlation analysis of [¹¹C]Ro15-4513 V_T values between each region pair across the HC group, with age and sex included as covariates. Next, a participant-level measure of difference was calculated for each non-HC participant. This was done by adding a single participant from the non-HC group to the HC reference group, and constructing another network as above. This new network was termed the “perturbed” network, in accordance with the nomenclature established by Liu et al. [44]. The difference between the perturbed network and the reference network was then calculated to obtain a differential network measure, denoted as ΔPCC . The null hypothesis was that ΔPCC_n is equal to the population mean of ΔPCC_n , and thus:

$$Z = \frac{\Delta PCC_n - \mu_{\Delta PCC}}{\sigma_{\Delta PCC}} = \frac{\Delta PCC_n}{\frac{1 - PCC_n^2}{n-1}}$$

Where n denotes the total number of participants in the reference group, while $\mu_{\Delta PCC}$ and $\sigma_{\Delta PCC}$ are the mean and standard deviation of the differential network ΔPCC . It can be shown that for sufficiently large n (previously indicated as at least 28 participants [73]), the mean and the standard deviation of ΔPCC_n for the population are $\mu_{\Delta PCC} = 0$ and $\sigma_{\Delta PCC} = 1 - PCC_n^2/n - 1$ [44]. Thus, the Z matrix essentially represents the level of abnormality in the covariance, where each edge exhibits a level of variation in molecular availability, leading to deviations from the values observed in the reference group. The p-value for each edge can be derived from the z-scores [44]. For the HC group, participant-level connectivity matrix was calculated by removing one HC participant at a time (i.e., by jackknife resampling), as done previously [74]. Data points identified as outliers (see ‘PET data quantification and quality checks’ above) were

Table 1. Demographic and clinical characteristics of the study sample.

	Control (n = 23) n	CHRp (n = 22)	FEP (n = 10)	χ^2/F	p
Female/Male	14/9	15/7	3/7	4.2	0.120
Ethnicity					
White	7	13	3	-	-
Black	2	5	5	-	-
Asian	10	0	0	-	-
Mixed or multiple	2	3	2	-	-
Other	2	1	0	-	-
	mean (SD)			F	p
Age	25.1 (4.5)	25.1 (4.6)	29 (3.6)	3.3	0.046
CAARMS					
Positive	2 (2.1)	12.7 (2.7)	-	-	-
Negative	0.8 (1.5)	7.1 (4.4)	-	-	-
PANSS					
Positive	-	-	17.5 (2.6)	-	-
Negative	-	-	14.9 (6)	-	-
Composite	-	-	2.6 (6.6)	-	-
General	-	-	27.8 (3.4)	-	-
HAM-A	3.8 (2.7)	17.6 (10.1)	10.8 (6.3)	19.4	<0.001
HAM-D	2.4 (1.8)	12.5 (6.4)	8.8 (4.8)	24.7	<0.001
AP (CPZ, mg)	-	-	204.3 (141.9)	-	-
GF:S	8.2 (1.2)	6.7 (1.6)	6.2 (1.6)	8.7	<0.001
GF:R	8.4 (1.1)	6.9 (1.8)	6.1 (1.4)	10.8	<0.001

GF:S and GF:R scores were missing for two control participants. HAM-A and HAM-D scores were missing for two control participants. Negative CAARMS scores were missing for 10 control participants. Antipsychotic medication dose presented as chlorpromazine equivalents for the seven FEP participants who were taking medication at the time of study. Missing data points were omitted in summary or statistics.

CHRp clinical high risk for psychosis, FEP first episode of psychosis, SD standard deviation, CAARMS comprehensive assessment for at-risk mental states (positive items: 1.1.Unusual Thought Content, 1.2.Non-Bizarre Ideas, 1.3.Perceptual Abnormalities, 1.4.Disorganised Speech; negative items: 4.1.Alogia, 4.2.Avolition/Apathy, 4.3.Anhedonia), PANSS positive and negative syndrome scale (positive items: P1-P7; negative items: N1-N7; general items: G1-G16; composite score: negative score subtracted from the positive score), HAM-A/D hamilton anxiety/depression scale, AP antipsychotic, CPZ chlorpromazine, GF:S/R global functioning social/role scale.

imputed using the mean of the ROI values across all other participants [75]. Values were imputed for three HC (for parahippocampal gyrus, nucleus accumbens and anterior cingulate, respectively) and for one CHRp participant (nucleus accumbens).

Between-group differences in regional [¹¹C]Ro15-4513 binding covariance

Statistical comparisons of the distribution of these deviation measures (z-scores) were conducted using a 1000-permutation test, wherein the null distribution was estimated by permuting group labels. The magnitude of the effect was quantified using Cohen's *d* effect size, appropriate for pairwise comparisons. Lower triangular matrices across groups were used for this analysis to exclude duplicate z-score values. These differences were first evaluated across all brain regions, and subsequently only for correlations between the hippocampus and other brain regions. Additionally, the proportion of extreme deviations at the region level was computed for each participant, a metric indicating deviation patterns at the regional level, and statistically compared between groups using a 1000-permutation test. As the z-score measures and the regional extreme deviations produced similar statistical results, the analysis using z-scores is reported in the main text, while the other is presented in the Supplement for completeness (Supplementary Methods and Results: Regional extreme deviations analysis, Supplementary Fig. 3). Additionally, group classification based on covariance networks was performed with a Cubic Support Vector Machine model; this is also reported in the Supplement (Supplementary Methods and Results: Group classification by regional [¹¹C]Ro15-4513 binding covariance, Supplementary Fig. 4).

RESULTS

Demographic and clinical data

Three participants were excluded: one CHRp participant due to missing arterial blood data, one further CHRp participant due to incomplete PET acquisition, and one HC participant due to an error in blood data processing. The resulting final study sample was n(CHRp) = 22, n(HC) = 23, n(FEP) = 10. There was no significant difference in sex between groups ($\chi^2 = 4.2$, $p = 0.12$). There was a significant difference in age between groups ($F(2,52) = 3.3$, $p = 0.046$, $ges = 0.11$), in that FEP participants were older than the other two groups; however, the results did not survive multiple comparison correction (Supplementary Table 1). There was also a significant difference in reported anxiety and depression between groups (anxiety: $F(2,50) = 19.4$, $p < 0.001$, $ges = 0.44$; depression: $F(2,50) = 24.7$, $p < 0.001$, $ges = 0.50$), where CHRp participants reported more symptoms of anxiety and depression than FEP and HC participants, and FEP participants reported more symptoms of anxiety and depression than HC (Supplementary Table 1). There was also a significant difference in reported social and role functioning between groups (GF:S: $F(2,50) = 8.7$, $p < 0.001$, $ges = 0.26$; GF:R: $F(2,50) = 10.8$, $p < 0.001$, $ges = 0.30$), where CHRp and FEP participants reported worse functioning than HC on both subscales (Supplementary Table 1). Participant's demographic and clinical data is summarised in Table 1.

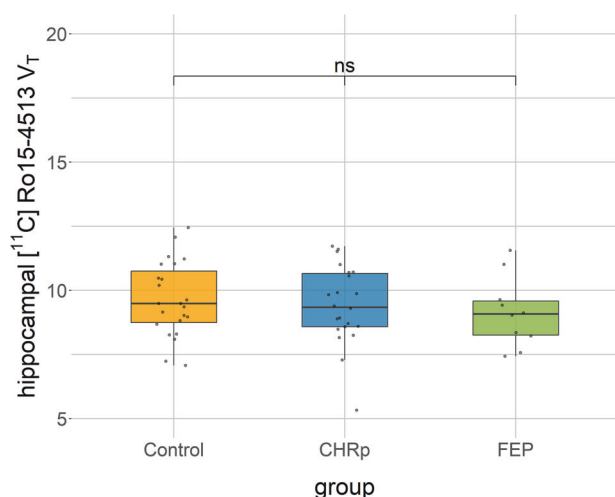


Fig. 1 [^{11}C]Ro15-4513 binding in the hippocampus between groups. CHRp, clinical high risk for psychosis; FEP, first episode of psychosis; ns, not significant; V_T , total volume of distribution.

Hippocampal [^{11}C]Ro15-4513 binding

There was no significant difference in hippocampal [^{11}C]Ro15-4513 binding between groups (one-way ANOVA with sex and age as covariates of no interest: $F(2,50) = 0.25$, $p = 0.78$, $g_{\text{es}} = 0.01$) (Fig. 1) or between the CHRp and HC groups, specifically (Supplementary Results: Hippocampal [^{11}C]Ro15-4513 binding).

Hippocampal [^{11}C]Ro15-4513 binding was not correlated with positive and negative psychosis symptoms or anxiety in the CHRp group. In the FEP group, it was correlated with the severity of negative symptoms (Pearson's $r = -0.65$, $p = 0.04$). However, this finding was no longer significant after covarying for antipsychotic dose (Pearson's $r = -0.64$, $p = 0.06$). There were no other significant correlations between hippocampal V_T and PANSS-positive, anxiety or depression symptoms. In HC, binding was correlated with levels of positive and negative psychosis symptoms and anxiety. The findings are comprehensively reported in Supplementary Results: Hippocampal [^{11}C]Ro15-4513 binding.

Brain-wide [^{11}C]Ro15-4513 binding

A supplementary analysis of [^{11}C]Ro15-4513 binding between study groups across all regions tested showed a significant difference between groups (mixed ANOVA with sex and age as covariates of no interest: $F(2,50) = 3.5$, $p = 0.039$, $g_{\text{es}} = 0.006$) and a potential group*region interaction ($F(44,1100) = 2.3$, $p < 0.001$, $p_{\text{GG}} = 0.097$, $g_{\text{es}} = 0.08$) (for average binding estimates, see Supplementary Table 2). Pairwise analyses across regions revealed a significant difference between the HC and FEP groups (main effect of group: $F(1,29) = 7.8$, $p < 0.001$, $p_{\text{Bonferroni}} < 0.001$, $g_{\text{es}} = 0.01$) that was region-dependent (group*region interaction: $F(22,638) = 5.2$, $p < 0.001$, $p_{\text{Bonferroni}} < 0.001$, $p_{\text{GG}} = 0.02$, $g_{\text{es}} = 0.15$). Post-hoc pairwise comparisons revealed this was driven by lower [^{11}C]Ro15-4513 binding in the nucleus accumbens in FEP participants than in the HC group ($F(1,29) = 6.0$, $p = 0.02$, $g_{\text{es}} = 0.17$), although this result did not survive Bonferroni correction ($p_{\text{Bonferroni}} = 0.46$) (Supplementary Table 3; Supplementary Fig. 1). The overall main effect of group was not significant after the addition of recent caffeine, tobacco, alcohol and cannabis use in the analysis (Supplementary Methods and Results: Effects of recent substance use on regional and brain-wide [^{11}C]Ro15-4513 binding).

There was no significant difference between the CHRp and FEP groups across all regions tested (main effect of group: $F(1,28) = 0.006$, $p = 0.94$, $g_{\text{es}} = 0.00009$). The findings remained unchanged after adding caffeine, tobacco, alcohol and cannabis use as covariates of no interest (Supplementary Results: Effects of

recent substance use on [^{11}C]Ro15-4513 binding covariance). There was a potential group*region interaction ($F(22,616) = 1.9$, $p = 0.007$, $p_{\text{Bonferroni}} = 0.021$, $p_{\text{GG}} = 0.17$, $g_{\text{es}} = 0.04$), but pairwise post-hoc comparisons did not reveal any region-specific significant differences between the two groups (Supplementary Table 4).

There was no significant difference in [^{11}C]Ro15-4513 binding between the HC and CHRp groups across all regions (main effect of group: $F(1,41) = 2.1$, $p = 0.16$, $g_{\text{es}} = 0.002$; group*region interaction: $F(22,902) = 1.0$, $p = 0.44$, $p_{\text{GG}} = 0.3$, $g_{\text{es}} = 0.023$).

Between-group differences in [^{11}C]Ro15-4513 binding network covariance

1 000-permutation tests showed significant differences in z-score distributions across all brain regions between HC and FEP ($p < 0.001$, Cohen's $d = 0.5$), between HC and CHRp ($p < 0.001$, Cohen's $d = 0.2$), but not between FEP and CHRp ($p = 0.7$, Cohen's $d = 0.06$). Similar differences were observed when focusing exclusively on the hippocampus, between HC and FEP ($p < 0.001$, Cohen's $d = 0.67$), and HC and CHRp ($p < 0.001$, Cohen's $d = 0.26$), but not between FEP and CHRp ($p = 0.34$, Cohen's $d = 0.07$) (Fig. 2). The findings were similar after adding caffeine, tobacco, alcohol and cannabis use as covariates of no interest (Supplementary Results: The effect of recent substance use on [^{11}C]Ro15-4513 binding covariance). Average z-score matrices across participants in the CHRp and FEP groups can be found in Supplementary Fig. 2. These results indicate that the [^{11}C]Ro15-4513 binding covariance perturbation network of CHRp individuals exhibited significant negative deviations from HC at a whole-brain level, though to a lesser extent than those with an FEP. Moreover, the FEP group demonstrated more pronounced negative deviations, particularly in the hippocampus, suggesting a potential reduction in covariance between the hippocampus and other brain regions (Supplementary Fig. 2).

DISCUSSION

The present study found that while hippocampal GABA_ARα5 availability did not differ between groups, brain-wide and hippocampal GABA_ARα5 covariance patterns were decreased in both CHRp and FEP individuals compared to HC. These findings suggest that individuals at clinical high-risk for psychosis and people with early psychosis may show alterations to the brain-wide organisation of the GABA_ARα5 system, rather than changes at a regional level.

Our findings build upon previous research investigating GABAergic function in psychosis, both at the microcircuit and whole-brain levels. Initial evidence for a GABAergic dysfunction in psychosis came from post-mortem studies in schizophrenia. These studies showed non-pyramidal cell reductions in the hippocampus [76], specifically the parvalbumin-positive (PVALB+) inhibitory interneurons [2, 3]. Similarly, a disruption in hippocampal development in the MAM model led to local Pvalb+ interneuron loss [14, 15], GABA_ARα5 density decrease across the hippocampus [25], subcortical hyperdopaminergia and behavioural changes of relevance for schizophrenia [14, 16]. These psychosis-relevant phenotypes in MAM-treated rats were prevented by peripubertal benzodiazepine administration, and normalised by direct infusion of a GABA_ARα5 positive allosteric modulator into the hippocampus [21, 22, 24]. The present study sought to forward-translate these findings by investigating GABA_ARα5 availability in individuals at CHRp and with an FEP.

Contrary to our hypothesis, we found no evidence of alterations in [^{11}C]Ro15-4513 binding in CHRp or FEP individuals compared to HC, either in the hippocampus or across the brain. To our knowledge, this is the first [^{11}C]Ro15-4513 study in the CHRp population. The CHRp group was well-powered, making it unlikely for sample size to explain the null finding. These results may

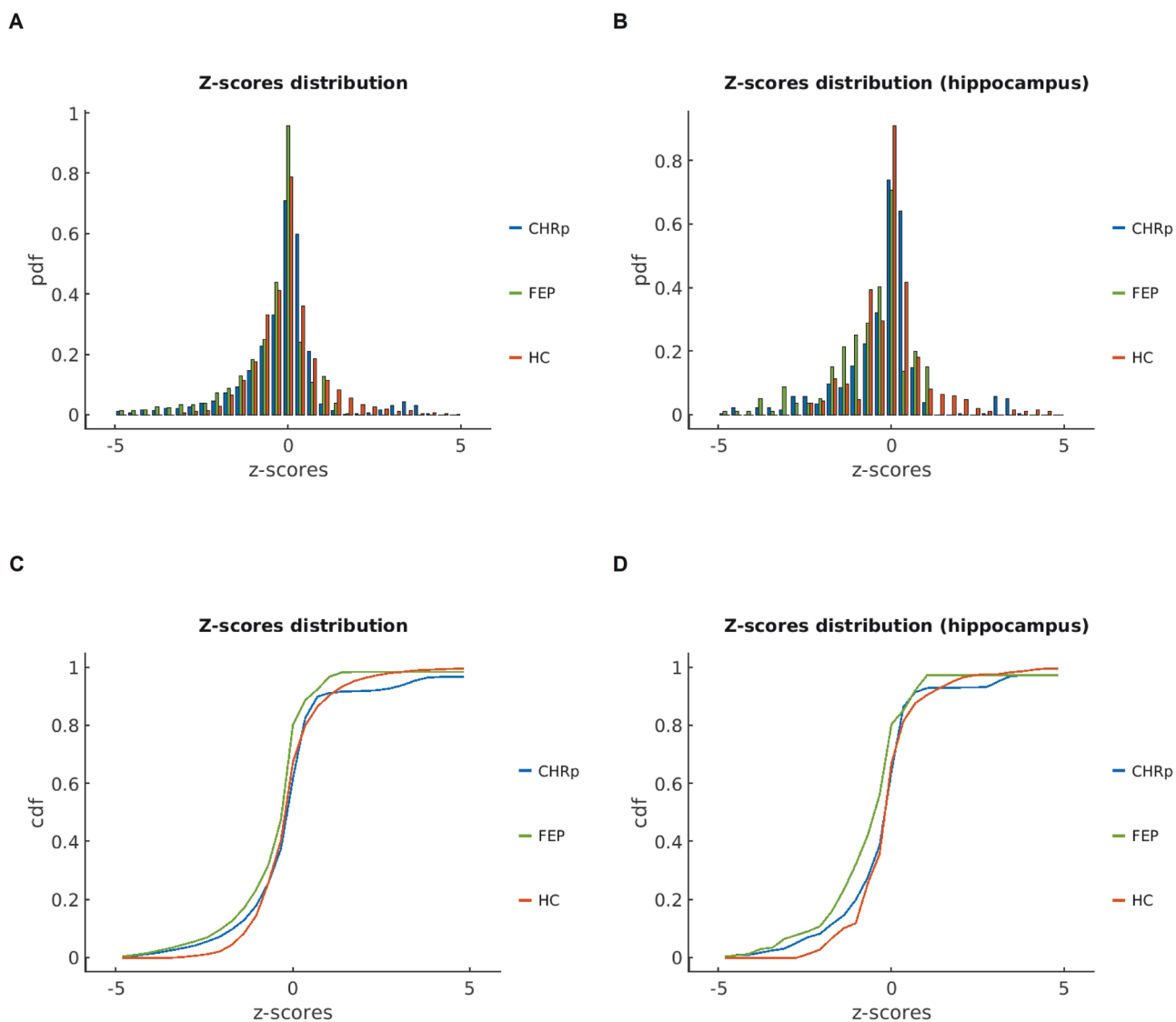


Fig. 2 Perturbation covariance z-score statistics. Probability density function (PDF) of z-score distributions between healthy controls (HC), individuals at clinical high-risk for psychosis (CHRp) and people with a first episode of psychosis (FEP), across the whole brain (A) and focusing on correlations with the hippocampus only (B). Cumulative distribution function (CDF) of z-scores from the lower triangular matrices for HC, CHRp and FEP across the whole brain (C) and focusing specifically on the hippocampus (D).

suggest that systematic alterations in regional GABA_ARα5 availability are not present in CHRp individuals. However, regional GABA_ARα5 deficits might only be present in a subgroup of CHRp individuals who subsequently develop psychosis. Although our sample was not large enough to investigate this, two previous studies addressed this question using less selective compounds. A recent study showed that normative GABA_AR availability was not associated with brain perfusion differences between CHRp individuals with different transition status [77]. Additionally, a retrospective analysis in over 500 CHRp individuals found no association between benzodiazepine exposure and psychosis transition risk [78]. While this may suggest that general GABAergic function might not be a predictor of transition, future longitudinal studies using compounds specific to individual GABAergic system components are needed to elucidate this.

While we found no evidence of a difference in [¹¹C]Ro15-4513 binding in the hippocampus of individuals with an FEP compared to HC, one previous [¹¹C]Ro15-4513 study reported lower regional GABA_ARα5 availability in the hippocampus of ten antipsychotic-free patients with schizophrenia [38]. In contrast, another previous

study with eleven participants (both medicated and medication-free) did not find such a difference [37]. As all studies to date have involved small numbers of participants, further investigation in larger samples is warranted. Nevertheless, it is plausible that changes in regional GABA_ARα5 availability may not be present in patients currently on antipsychotic medication. This is partly consistent with preclinical evidence showing increases in GABA_ARα5 availability following antipsychotic exposure [79], and a proton magnetic resonance spectroscopy (¹H-MRS) study which reported normalised GABA levels in the anterior cingulate cortex of medication-naïve schizophrenia patients after antipsychotic treatment [80]. Further research directly comparing larger participant samples with and without antipsychotic treatment is required to expand on these findings. Such investigations in human participants in vivo would also circumvent limitations of post-mortem studies, such as disorder chronicity and effects of death.

Reviewing the common GABAergic interneuron-receptor subtype associations may also help understand the findings from port-mortem examinations in schizophrenia, which provided the

central evidence towards GABAergic dysfunction in psychosis. PVALB+ inhibitory interneurons most commonly synapse onto $\alpha 1$ subunit-containing GABA_AR_s, whereas GABA_AR₅s are expressed in proximity to somatostatin (SST)-expressing interneurons [23, 81–83]. Previous research showed that about 66% of [¹¹C]Ro15-4513 signal represents GABA_AR₅ binding [70]. In our previous imaging transcriptomics study, we found that [¹¹C]Ro15-4513 binding tracked the expression of *GABRA5* and *SST*, and covaried negatively with *PVALB* expression [32]. This may suggest that [¹¹C]Ro15-4513 PET, tracking GABA_AR₅s and SST+ inhibitory interneurons more likely than PVALB+ interneurons, may not be optimal for capturing alterations in the GABAergic microcircuits posited to be predominantly involved in psychosis symptom emergence by port-mortem examinations. However, it is plausible that a loss of PVALB+ interneurons may lead to regional GABA_AR₅ upregulation to compensate for a decrease in inhibition. Alternatively, any alterations in GABA_AR₅ expression may be compensated by changes in the levels of other GABA_AR_s that [¹¹C]Ro15-4513 binds to. Further research using novel radiotracers and other techniques such as in vitro cultures of interneurons is required to elucidate this question.

Our second hypothesis was that CHRp and FEP individuals would exhibit significant deviations in GABA_AR₅ network covariance relative to the normative healthy control group, both brain-wide and when focusing on the hippocampus, consistent with the notion that the hippocampus may play a key role in psychosis [19, 84]. Accordingly, we identified significant covariance decrease in GABA_AR₅ availability in CHRp and FEP compared to HC individuals across brain regions, which was also present for the hippocampus. This was indicated by an average decrease in covariance after the addition of a participant from either of these groups to the reference group. These results are broadly consistent with previous studies on brain functional and structural variability in schizophrenia. For example, a recent study employing a normative modelling approach found increased variability in brain structure in schizophrenia [85]. At the temporal scale, there is robust meta-analytic evidence for altered resting-state functional connectivity across the psychosis spectrum [e.g., [85–87]]. Moreover, several meta-analyses have found alterations in the brain-wide pattern of regional hyper- and hypoactivations in schizophrenia [88–91]. Overall, these results suggest that alterations in the organisation of the GABA_AR₅ system, both across the brain and between the hippocampus and other brain regions, may be involved in clinical high-risk and early psychosis, which aligns with the dysconnectivity hypothesis of schizophrenia [41]. It is plausible that this dysregulation contributes to the previously observed hippocampal hyperactivity. However, it is less well understood what molecular mechanisms may underlie such phenomenon. Future research should address this by investigating the relationships between GABA_AR₅ system organisation and other biological processes, such as glutamatergic neurotransmission.

There are several strengths of this study. Importantly, this is the first study investigating GABA_AR₅ availability in people at CHRp, for which we reached a sample size indicated by our power calculation. Additionally, we employed full tracer kinetic quantification and an additional molecular covariance approach to comprehensively characterise brain-wide GABA_AR₅ availability. Nevertheless, we did not reach the participant number indicated by power calculation in the FEP group, limiting the interpretability of these results. Further, we cannot exclude secondary binding to other targets by the radiotracer we employed. Pharmacological competition studies showed that even in regions rich in GABA_AR₅ expression, this receptor subtype accounts for 60–70% of all local [¹¹C]Ro15-4513 binding [70]. Additionally, our [¹¹C]Ro15-4513 binding covariance perturbation analyses relied on comparisons with the HC group using metrics derived from the HC group. As such, our results need to be corroborated by a similar study comparing a HC

group alongside a CHRp and FEP sample with an independent reference HC group. Finally, we were not able to investigate if binding was related to clinical outcomes in CHRp individuals (such as transition to psychosis) because the sample size was too small.

Our findings suggest that individuals at CHRp and with an FEP show lower brain-wide GABA_AR₅ system covariance, but no regional availability alterations in the hippocampus. These findings support the utility of constructing individualised meta-bolic abnormality networks derived from single participant scans across the extended psychosis spectrum.

DATA AVAILABILITY

The positron emission tomography data are freely available at: <https://doi.org/10.6084/m9.figshare.30022447>. Any other data is available from the corresponding author on reasonable request.

CODE AVAILABILITY

Any custom code underlying the presented analysis is available from the corresponding author on reasonable request.

REFERENCES

1. Benes FM, Kwok EW, Vincent SL, Todtenkopf MS. A reduction of nonpyramidal cells in sector CA2 of schizophrenics and manic depressives. *Biol Psychiatry*. 1998;44:88–97. [https://doi.org/10.1016/S0006-3223\(98\)00138-3](https://doi.org/10.1016/S0006-3223(98)00138-3)
2. Zhang ZJ, Reynolds GP. A selective decrease in the relative density of parvalbumin-immunoreactive neurons in the hippocampus in schizophrenia. *Schizophr Res*. 2002;55:1–10. [https://doi.org/10.1016/S0920-9964\(01\)00188-8](https://doi.org/10.1016/S0920-9964(01)00188-8)
3. Konradi C, Yang CK, Zimmerman EI, Lohmann KM, Gresch P, Pantazopoulos H, et al. Hippocampal interneurons are abnormal in schizophrenia. *Schizophr Res*. 2011;131:165–73. <https://doi.org/10.1016/J.SCHRES.2011.06.007>
4. Tamminga CA, Stan AD, Wagner AD. The hippocampal formation in schizophrenia. *Am J Psychiatry*. 2010;167:1178–93. <https://doi.org/10.1176/APPI.AJP.2010.09081187>
5. Talati P, Rane S, Skinner J, Gore J, Heckers S. Increased hippocampal blood volume and normal blood flow in schizophrenia. *Psychiatry Res*. 2015;232:219. <https://doi.org/10.1016/J.PSYCHRES.2015.03.007>
6. Allen P, Chaddock CA, Egerton A, Howes OD, Bonoldi I, Yelaya F, et al. Resting hyperperfusion of the hippocampus, midbrain, and basal ganglia in people at high risk for psychosis. *Am J Psychiatry*. 2016;173:392–9. <https://doi.org/10.1176/APPI.AJP.2015.15040485>
7. Schobel SA, Chaudhury NH, Khan UA, Paniagua B, Styner MA, Asllani I, et al. Imaging patients with psychosis and a mouse model establishes a spreading pattern of hippocampal dysfunction and implicates glutamate as a driver. *Neuron*. 2013;78:81–93. <https://doi.org/10.1016/J.NEURON.2013.02.011>
8. Modinos G, Şimşek F, Aziz M, Bossong M, Bonoldi I, Samson C, et al. Prefrontal GABA levels, hippocampal resting perfusion and the risk of psychosis. *Neuropsychopharmacology*. 2018;43:2652. <https://doi.org/10.1038/S41386-017-0004-6>
9. Ruhrmann S, Schultze-Lutter F, Salokangas RKR, Heinimaa M, Linszen D, Dingemans P, et al. Prediction of psychosis in adolescents and young adults at high risk: results from the prospective European prediction of psychosis study. *Arch Gen Psychiatry*. 2010;67:241–51. <https://doi.org/10.1001/ARCHGENPSYCHIATRY.2009.206>
10. Keshavan MS, DeLisi LE, Seidman LJ. Early and broadly defined psychosis risk mental states. *Schizophr Res*. 2011;126:1–10. <https://doi.org/10.1016/J.SCHRES.2010.10.006>
11. Fusar-Poli P. The Clinical High-Risk state for Psychosis (CHR-P), version II. *Schizophr Bull*. 2017;43:44–7. <https://doi.org/10.1093/SCHBUL/SBW158>
12. Salazar De Pablo G, Radua J, Pereira J, Bonoldi I, Arienti V, Besana F, et al. Probability of transition to psychosis in individuals at clinical high risk: an updated meta-analysis. *JAMA Psychiatry*. 2021;78:970–8. <https://doi.org/10.1001/JAMAPSYCHIATRY.2021.0830>
13. Moore H, Jentsch JD, Ghajarnia M, Geyer MA, Grace AA. A neurobehavioral systems analysis of adult rats exposed to methylazoxymethanol acetate on E17: implications for the neuropathology of schizophrenia. *Biol Psychiatry*. 2006;60:253–64. <https://doi.org/10.1016/J.BIOPSYCH.2006.01.003>
14. Lodge DJ, Grace AA. Aberrant hippocampal activity underlies the dopamine dysregulation in an animal model of schizophrenia. *J Neurosci*. 2007;27:11424–30. <https://doi.org/10.1523/JNEUROSCI.2847-07.2007>
15. Goto Y, Grace AA. Alterations in medial prefrontal cortical activity and plasticity in rats with disruption of cortical development. *Biol Psychiatry*. 2006;60:1259–67. <https://doi.org/10.1016/J.BIOPSYCH.2006.05.046>

16. Howes OD, Kapur S. The dopamine hypothesis of schizophrenia: version III—the final common pathway. *Schizophr Bull.* 2009;35:549–62. <https://doi.org/10.1093/SCHBUL/SBP006>
17. Egerton A, Chaddock CA, Winton-Brown TT, Bloomfield MAP, Bhattacharyya S, Allen P, et al. Presynaptic striatal dopamine dysfunction in people at ultra-high risk for psychosis: findings in a second cohort. *Biol Psychiatry.* 2013;74:106–12. <https://doi.org/10.1016/J.BIOPSYCH.2012.11.017>
18. Pennartz CMA, Ito R, Verschure PFMJ, Battaglia FP, Robbins TW. The hippocampal–striatal axis in learning, prediction and goal-directed behavior. *Trends Neurosci.* 2011;34:548–59. <https://doi.org/10.1016/J.TINS.2011.08.001>
19. Grace AA. Dysregulation of the dopamine system in the pathophysiology of schizophrenia and depression. *Nat Rev Neurosci.* 2016;17:524. <https://doi.org/10.1038/NRN.2016.57>
20. Modinos G, Allen P, Grace AA, McGuire P. Translating the MAM model of psychosis to humans. *Trends Neurosci.* 2015;38:129–38. <https://doi.org/10.1016/J.TINS.2014.12.005>
21. Lodge DJ, Behrens MM, Grace AA. A loss of parvalbumin-containing interneurons is associated with diminished oscillatory activity in an animal model of schizophrenia. *J Neurosci.* 2009;29:2344–54. <https://doi.org/10.1523/JNEUROSCI.5419-08.2009>
22. Du Y, Grace AA. Amygdala hyperactivity in MAM model of schizophrenia is normalized by peripubertal diazepam administration. *Neuropsychopharmacology.* 2016;41:2455–62. <https://doi.org/10.1038/NPP.2016.42>
23. Rudolph U, Möhler H. GABA-based therapeutic approaches: GABA_A receptor subtype functions. *Curr Opin Pharmacol.* 2006;6:18–23. <https://doi.org/10.1016/J.COHP.2005.10.003>
24. Gill KM, Lodge DJ, Cook JM, Aras S, Grace AA. A novel α 5GABA_A-positive allosteric modulator reverses hyperactivation of the dopamine system in the MAM model of schizophrenia. *Neuropsychopharmacology.* 2011;36:1903. <https://doi.org/10.1038/NPP.2011.76>
25. Kiemes A, Gomes FV, Cash D, Uliana DL, Simmons C, Singh N, et al. GABA_A and NMDA receptor density alterations and their behavioral correlates in the gestational methylazoxymethanol acetate model for schizophrenia. *Neuropsychopharmacology.* 2021;47:687–95. <https://doi.org/10.1038/s41386-021-01213-0>
26. Sieghart W, Sperk G. Subunit composition, distribution and function of GABA(A) receptor subtypes. *Curr Top Med Chem.* 2002;2:795–816. <https://doi.org/10.2174/1568026023393507>
27. Brickley SG, Mody I. Extrasynaptic GABA_A receptors: their function in the CNS and implications for disease. *Neuron.* 2012;73:23. <https://doi.org/10.1016/J.NEURON.2011.12.012>
28. Glykys J, Mody I. Activation of GABA_A receptors: views from outside the synaptic cleft. *Neuron.* 2007;56:763–70. <https://doi.org/10.1016/J.NEURON.2007.11.002>
29. Squires RF, Lajtha A, Saederup E, Palkovits M. Reduced [3H]flunitrazepam binding in cingulate cortex and hippocampus of postmortem schizophrenic brains: is selective loss of glutamatergic neurons associated with major psychoses? *Neurochem Res.* 1993;18:219–23. <https://doi.org/10.1007/BF01474687>
30. Reynolds GP, Stroud D. Hippocampal benzodiazepine receptors in schizophrenia. *J Neural Transm Gen Sect.* 1993;93:151–5. <https://doi.org/10.1007/BF01245344>
31. Kiuchi Y, Kobayashi T, Takeuchi J, Shimizu H, Ogata H, Toru M. Benzodiazepine receptors increase in post-mortem brain of chronic schizophrenics. *Eur Arch Psychiatry Neurol Sci.* 1989;239:71–8. <https://doi.org/10.1007/BF01759578>
32. Lukow PB, Martins D, Veronese M, Vernon AC, McGuire P, Turkheimer FE, et al. Cellular and molecular signatures of in vivo imaging measures of GABAergic neurotransmission in the human brain. *Commun Biol.* 2022;5:372. <https://doi.org/10.1038/s42003-022-03268-1>
33. Egerton A, Modinos G, Ferrera D, McGuire P. Neuroimaging studies of GABA in schizophrenia: a systematic review with meta-analysis. *Transl Psychiatry.* 2017;7:e1147. <https://doi.org/10.1038/TP.2017.124>
34. Lingford-Hughes A, Hume SP, Feeney A, Hirani E, Osman S, Cunningham VJ, et al. Imaging the GABA-benzodiazepine receptor subtype containing the α 5-subunit in vivo with [11C]Ro15 4513 positron emission tomography. *J Cereb Blood Flow Metab.* 2002;22:878–89. <https://doi.org/10.1097/00004647-200207000-00013>
35. Frankle WG, Cho RY, Prasad KM, Mason NS, Paris J, Himes ML, et al. In vivo measurement of GABA transmission in healthy subjects and schizophrenia patients. *Am J Psychiatry.* 2015;172:1148. <https://doi.org/10.1176/APPI.AJP.2015.14081031>
36. Lee JS, Lee JD, Park H-J, Oh M-K, Chun JW, Kim S-J, et al. Is the GABA system related to the social competence improvement effect of aripiprazole? An 18F-Fluorofluzazenil PET study. *Psychiatry Investig.* 2013;10:75. <https://doi.org/10.4306/PI.2013.10.1.75>
37. Asai Y, Takano A, Ito H, Okubo Y, Matsuura M, Otsuka A, et al. GABA_A/Benzodiazepine receptor binding in patients with schizophrenia using [11C]Ro15-4513, a radioligand with relatively high affinity for α 5 subunit. *Schizophr Res.* 2008;99:333–40. <https://doi.org/10.1016/J.SCHRES.2007.10.014>
38. Marques TR, Ashok AH, Angelescu I, Borgan F, Myers J, Lingford-Hughes A, et al. GABA-A receptor differences in schizophrenia: a positron emission tomography study using [11C]Ro154513. *Mol Psychiatry.* 2020;26:2616–25. <https://doi.org/10.1038/s41380-020-0711-y>
39. Kang JI, Park HJ, Kim SJ, Kim KR, Lee SY, Lee E, et al. Reduced binding potential of GABA-A/benzodiazepine receptors in individuals at ultra-high risk for psychosis: an [18F]-fluorofluzazenil positron emission tomography study. *Schizophr Bull.* 2014;40:548–57. <https://doi.org/10.1093/SCHBUL/SBT052>
40. Zhu S, Noviello CM, Teng J, Walsh RM, Kim JJ, Hibbs RE. Structure of a human synaptic GABA_A receptor. *Nature.* 2018;559:67–88. <https://doi.org/10.1038/S41586-018-0255-3>
41. Friston K, Brown HR, Siemerker J, Stephan KE. The dysconnection hypothesis (2016). *Schizophr Res.* 2016;176:83–94. <https://doi.org/10.1016/J.SCHRES.2016.07.014>
42. Sun T, Wang Z, Wu Y, Gu F, Li X, Bai Y, et al. Identifying the individual metabolic abnormalities from a systemic perspective using whole-body PET imaging. *Eur J Nucl Med Mol Imaging.* 2022;49:2994–3004. <https://doi.org/10.1007/S00259-022-05832-7/FIGURES/7>
43. Sala A, Lizarraga A, Caminiti SP, Calhoun VD, Eickhoff SB, Habeck C, et al. Brain connectomics: time for a molecular imaging perspective? *Trends Cogn Sci.* 2023;27:353–66. <https://doi.org/10.1016/J.TICS.2022.11.015>
44. Liu X, Wang Y, Ji H, Aihara K, Chen L. Personalized characterization of diseases using sample-specific networks. *Nucleic Acids Res.* 2016;44:e164–e164. <https://doi.org/10.1093/NAR/GKW772>
45. Fusar-Poli P, Spencer T, De Micheli A, Curzi V, Nandha S, McGuire P. Outreach and support in South-London (OASIS) 2001–2020: twenty years of early detection, prognosis and preventive care for young people at risk of psychosis. *Eur Neuropsychopharmacol.* 2020;39:111–22. <https://doi.org/10.1016/J.EURONEURO.2020.08.002>
46. Wechsler D. Administration and scoring manual for the Wechsler Adult Intelligence Scale (3rd ed., p 217). The Psychological Corporation; 1997.
47. Yung AR, Yung AR, Yuen HP, McGorry PD, Phillips LJ, Kelly D, et al. Mapping the onset of psychosis: the comprehensive assessment of at-risk mental states. *Aust N Z J Psychiatry.* 2005;39:964–71. <https://doi.org/10.1080/J.1440-1614.2005.01714.X>
48. Fusar-Poli P, Salazar de Pablo G, Rajkumar RP, López-Díaz Á, Malhotra S, Heckers S, et al. Diagnosis, prognosis, and treatment of brief psychotic episodes: a review and research agenda. *Lancet Psychiatry.* 2022;9:72–83. [https://doi.org/10.1016/S2215-0366\(21\)00121-8](https://doi.org/10.1016/S2215-0366(21)00121-8)
49. Fusar-Poli P, Cappucciati M, De Micheli A, Rutigliano G, Bonoldi I, Tognin S, et al. Diagnostic and prognostic significance of Brief Limited Intermittent Psychotic Symptoms (BLIPS) in individuals at ultra high risk. *Schizophr Bull.* 2017;43:48–56. <https://doi.org/10.1093/SCHBUL/SBW151>
50. Provenzani U, Salazar de Pablo G, Arribas M, Pillmann F, Fusar-Poli P. Clinical outcomes in brief psychotic episodes: a systematic review and meta-analysis. *Epidemiol Psychiatr Sci.* 2021;30:e71. <https://doi.org/10.1017/S2045796021000548>
51. Fusar-Poli P, Cappucciati M, Bonoldi I, Hui LMC, Rutigliano G, Stahl DR, et al. Prognosis of brief psychotic episodes: a meta-analysis. *JAMA Psychiatry.* 2016;73:211–20. <https://doi.org/10.1001/JAMAPSYCHIATRY.2015.2313>
52. World Health Organization. ICD-10 Version:2016. 2016. <https://icd.who.int/browse10/2016/en>.
53. Kay SR, Fiszbein A, Opler LA. The Positive and Negative Syndrome Scale (PANSS) for Schizophrenia. *Schizophr Bull.* 1987;13:261–76. <https://doi.org/10.1093/SCHBUL/13.2.261>
54. World Medical Association. World medical association declaration of Helsinki: ethical principles for medical research involving human subjects. *JAMA.* 2013;310:2191–4. <https://doi.org/10.1001/JAMA.2013.281053>
55. McGinnity CJ, Riaño Barros DA, Rosso L, Veronese M, Rizzo G, Bertoldo A, et al. Test-retest reproducibility of quantitative binding measures of [11C]Ro15-4513, a PET ligand for GABA_A receptors containing α 5 subunits. *Neuroimage.* 2017;152:270–82. <https://doi.org/10.1016/J.NEUROIMAGE.2016.12.038>
56. Hamilton M. The assessment of anxiety states by rating. *Br J Med Psychol.* 1959;32:50–5. <https://doi.org/10.1111/J.2044-8341.1959.TB00467.X>
57. Hamilton M. A rating scale for depression. *J Neurol Neurosurg Psychiatry.* 1960;23:56–62. <https://doi.org/10.1136/JNPP.23.1.56>
58. Carrión RE, Auther AM, McLaughlin D, Olsen R, Addington J, Bearden CE, et al. The global functioning: social and role scales—further validation in a large sample of adolescents and Young Adults at clinical high risk for psychosis. *Schizophr Bull.* 2019;45:763–72. <https://doi.org/10.1093/SCHBUL/SBY126>
59. Woods SW. Chlorpromazine equivalent doses for the newer atypical antipsychotics. *J Clin Psychiatry.* 2003;64:2601.
60. Leucht S, Crippa A, Sifias S, Patel MX, Orsini N, Davis JM. Dose-response meta-analysis of antipsychotic drugs for acute schizophrenia. *Am J Psychiatry.* 2020;177:342–53. https://doi.org/10.1176/APPI.AJP.2019.19010034/SUPPL_FILE/APPI.AJP.2019.19010034.DS001.PDF
61. Leucht S, Samara M, Heres S, Davis JM. Dose equivalents for antipsychotic drugs: The DDD method. *Schizophr Bull.* 2016;42:590–4. <https://doi.org/10.1093/SCHBUL/SBV167>
62. Gardner DM, Murphy AL, O'Donnell H, Centorrino F, Baldessarini RJ. International consensus study of antipsychotic dosing. *Am J Psychiatry.* 2010;167:686–93. <https://doi.org/10.1176/APPI.AJP.2009.09060802/ASSET/IMAGES/0802TBL4.JPEG>

63. Davis JM. Dose equivalence of the anti-psychotic drugs. *J Psychiatr Res.* 1974;11:65–9. [https://doi.org/10.1016/0022-3956\(74\)90071-5](https://doi.org/10.1016/0022-3956(74)90071-5)
64. Field A, Miles J, Field Z. Discovering statistics using R – discovering statistics n.d. <https://discoveringstatistics.com/books/discovering-statistics-using-r/> (Accessed 30 Jul 2024).
65. Mazziotta JC, Toga AW, Evans A, Fox P, Lancaster J. A probabilistic atlas of the human brain: theory and rationale for its development: the International Consortium for Brain Mapping (ICBM). *Neuroimage.* 1995;2:89–101. <https://doi.org/10.1006/NIMG.1995.1012>
66. Tziortzi AC, Searle GE, Tzimopoulou S, Salinas C, Beaver JD, Jenkinson M, et al. Imaging dopamine receptors in humans with [¹¹C]-(+)-PHNO: dissection of D3 signal and anatomy. *Neuroimage.* 2011;54:264–77. <https://doi.org/10.1016/J.NEUROIMAGE.2010.06.044>
67. Horder J, Andersson M, Mendez MA, Singh N, Tangen Å, Lundberg J, et al. GABAA receptor availability is not altered in adults with autism spectrum disorder or in mouse models. *Sci Transl Med.* 2018;10:eam8434. <https://doi.org/10.1126/SCITRANSLMED.AAM8434>
68. Hammers A, Panagoda P, Heckemann RA, Kelsch W, Turkheimer FE, Brooks DJ, et al. [¹¹C]Flumazenil PET in temporal lobe epilepsy: do we need an arterial input function or kinetic modeling? *J Cereb Blood Flow Metab.* 2008;28:207–16. <https://doi.org/10.1038/SJ.CBFM.9600515>
69. Salinas CA, Searle GE, Gunn RN. The simplified reference tissue model: model assumption violations and their impact on binding potential. *J Cereb Blood Flow Metab.* 2014;35:304. <https://doi.org/10.1038/JCBFM.2014.202>
70. Myers JFM, Comley RA, Gunn RN. Quantification of [¹¹C]Ro15-4513 GABA_Aα5 specific binding and regional selectivity in humans. *J Cereb Blood Flow Metab.* 2017;37:2137–48. <https://doi.org/10.1177/0271678X16661339>
71. Innis RB, Cunningham VJ, Delforge J, Fujita M, Gjedde A, Gunn RN, et al. Consensus nomenclature for in vivo imaging of reversibly binding radioligands. *J Cereb Blood Flow Metab.* 2007;27:1533–9. <https://doi.org/10.1038/SJ.CBFM.9600493>
72. Ghasemi A, Zahediasl S. Normality tests for statistical analysis: a guide for non-statisticians. *Int J Endocrinol Metab.* 2012;10:486. <https://doi.org/10.5812/IJEM.3505>
73. Lu W, Song T, Li J, Zhang Y, Lu J. Individual-specific metabolic network based on 18F-FDG PET revealing multi-level aberrant metabolisms in Parkinson's disease. *Hum Brain Mapp.* 2024;45:e70026 <https://doi.org/10.1002/HBM.70026>
74. Han S, Zheng R, Li S, Zhou B, Jiang Y, Fang K, et al. Resolving heterogeneity in depression using individualized structural covariance network analysis. *Psychol Med.* 2023;53:5312–21. <https://doi.org/10.1017/S0033291722002380>
75. Donders ART, van der Heijden GJMG, Stijnen T, Moons KGM. Review: a gentle introduction to imputation of missing values. *J Clin Epidemiol.* 2006;59:1087–91. <https://doi.org/10.1016/J.JCLINEPI.2006.01.014>
76. Benes FM. Evidence for altered trisynaptic circuitry in schizophrenic hippocampus. *Biol Psychiatry.* 1999;46:589–99. [https://doi.org/10.1016/S0006-3223\(99\)00136-5](https://doi.org/10.1016/S0006-3223(99)00136-5)
77. Knight SR, Abbasova L, Zeighami Y, Hansen JY, Martins D, Zelaya F, et al. Transcriptional and neurochemical signatures of cerebral blood flow alterations in individuals with schizophrenia or at clinical high risk for psychosis. *Biol Psychiatry.* 2025;98:144–55. <https://doi.org/10.1016/j.biopsych.2025.01.028>
78. Livingston NR, De Micheli A, McCutcheon RA, Butler E, Hamdan M, Grace AA, et al. Effects of benzodiazepine exposure on real-world clinical outcomes in individuals at clinical high risk for psychosis. *Schizophr Bull.* 2024;51:446–57. <https://doi.org/10.1093/SCHBUL/SBAE036>
79. Peris-Yague A, Kiemes A, Cash D, Cotel MC, Singh N, Vernon AC, et al. Region-specific and dose-specific effects of chronic haloperidol exposure on [³H]-flumazenil and [³H]-Ro15-4513 GABA_A receptor binding sites in the rat brain. *Eur Neuropsychopharmacol.* 2020;41:106–17. <https://doi.org/10.1016/J.EURONEURO.2020.10.004>
80. de la Fuente-Sandoval C, Reyes-Madriral F, Mao X, León-Ortiz P, Rodríguez-Mayoral O, Jung-Cook H, et al. Prefrontal and striatal gamma-aminobutyric acid levels and the effect of antipsychotic treatment in first-episode psychosis patients. *Biol Psychiatry.* 2018;83:475–83. <https://doi.org/10.1016/J.BIOPSYCH.2017.09.028>
81. Pfeffer CK, Xue M, He M, Huang ZJ, Scanziani M. Inhibition of inhibition in visual cortex: the logic of connections between molecularly distinct interneurons. *Nat Neurosci.* 2013;16:1068–76. <https://doi.org/10.1038/NN.3446>
82. Hu H, Gan J, Jonas P. Fast-spiking, parvalbumin+ GABAergic interneurons: from cellular design to microcircuit function. *Science.* 2014;345:1255263. https://doi.org/10.1126/SCIENCE.1255263/ASSET/92DC2352-DFDF-4976-80AB-CFFD7869E6B1/ASSETS/GRAPHIC/345_1255263_F6.JPEG
83. Klausberger T, Roberts JDB, Somogyi P. Cell type- and input-specific differences in the number and subtypes of synaptic GABA(A) receptors in the hippocampus. *J Neurosci.* 2002;22:2513–21. <https://doi.org/10.1523/JNEUROSCI.22-07-02513.2002>
84. Knight S, McCutcheon R, Dwir D, Grace AA, O'Daly O, McGuire P, et al. Hippocampal circuit dysfunction in psychosis. *Transl Psychiatry.* 2022;12:344 <https://doi.org/10.1038/S41398-022-02115-5>
85. Liu Z, Palaniyappan L, Wu X, Zhang K, Du J, Zhao Q, et al. Resolving heterogeneity in schizophrenia through a novel systems approach to brain structure: individualized structural covariance network analysis. *Mol Psychiatry.* 2021;26:7719–31. <https://doi.org/10.1038/s41380-021-01229-4>
86. O'Neill A, Mechelli A, Bhattacharyya S. Dysconnectivity of large-scale functional networks in early psychosis: a meta-analysis. *Schizophr Bull.* 2019;45:579–90. <https://doi.org/10.1093/SCHBUL/SBY094>
87. Brandl F, Avram M, Weise B, Shang J, Simões B, Bertram T, et al. Specific substantial dysconnectivity in schizophrenia: a transdiagnostic multimodal meta-analysis of resting-state functional and structural magnetic resonance imaging studies. *Biol Psychiatry.* 2019;85:573–83. <https://doi.org/10.1016/J.BIOPSYCH.2018.12.003>
88. Li T, Wang Q, Zhang J, Rolls ET, Yang W, Palaniyappan L, et al. Brain-wide analysis of functional connectivity in first-episode and chronic stages of schizophrenia. *Schizophr Bull.* 2017;43:436–48. <https://doi.org/10.1093/SCHBUL/SBW099>
89. Gao Z, Xiao Y, Zhu F, Tao B, Yu W, Lui S. The whole-brain connectome landscape in patients with schizophrenia: a systematic review and meta-analysis of graph theoretical characteristics. *Neurosci Biobehav Rev.* 2023;148:105144. <https://doi.org/10.1016/J.NEUBIOREV.2023.105144>
90. Kambeitz J, Kambeitz-Ilankovic L, Cabral C, Dwyer DB, Calhoun VD, Van Den Heuvel MP, et al. Aberrant functional whole-brain network architecture in patients with schizophrenia: a meta-analysis. *Schizophr Bull.* 2016;42:S13–21. <https://doi.org/10.1093/SCHBUL/SBV174>
91. Crossley NA, Mechelli A, Ginestet C, Rubinov M, Bullmore ET, McGuire P. Altered hub functioning and compensatory activations in the connectome: a meta-analysis of functional neuroimaging studies in schizophrenia. *Schizophr Bull.* 2016;42:434–42. <https://doi.org/10.1093/SCHBUL/SBV146>

ACKNOWLEDGEMENTS

This research was funded by the Wellcome Trust & The Royal Society [Sir Henry Dale Fellowship 202397/Z/16/Z to GM]. This manuscript also represents independent research partly funded by the National Institute for Health and Care Research (NIHR) Maudsley Biomedical Research Centre (BRC) at South London and Maudsley NHS Foundation Trust and King's College London. PBL was in receipt of a PhD studentship funded by the NIHR Maudsley BRC. The views expressed are those of the author and not necessarily those of the NHS, the NIHR or the Department of Health and Social Care. AAG received funding from USPHS NIMH MH57440. MV is supported by EU funding within the MUR PNRR "National Center for HPC, BIG DATA AND QUANTUM COMPUTING (Project no. CN00000013 CN1), the Ministry of University and Research within the Complementary National Plan PNC DIGITAL LIFELONG PREVENTION - DARE (Project no PNC0000002_DARE), and by Fondo per il Programma Nazionale di Ricerca e Progetti di Rilevante Interesse Nazionale (PRIN, Project no 2022RKM3H7). The authors would like to thank Dr Zerrin Atakan for providing medical expertise during participant recruitment. For the purposes of open access, the author has applied a Creative Commons Attribution (CC BY) licence to any Accepted Author Manuscript version arising from this submission.

AUTHOR CONTRIBUTIONS

GM, PM and FET designed the research. GM obtained the funding. PBL, JJS, MS, SK, AK and NRL conducted the research. J Davies conducted neuroimaging data acquisition. AdM, TJS and PSP provided clinical oversight. BH, NV and J Donocik supported participant recruitment. EAR provided neuroimaging data acquisition oversight. MV and FET provided analytic support. PBL and MS wrote the original draft. PBL and MS made all figures. All authors critically revised the article. All authors approved the last version. Supervision was provided by GM, FET and PM.

COMPETING INTERESTS

AAG has received consulting fees from Alkermes, Lundbeck, Takeda, Roche, Lyra, Concert, Newron and SynAgile, and research funding from Lundbeck, Newron and Merck. EAR is a full-time employee of Invicro. MV is named as an inventor on a patent related to the use of dopaminergic imaging in mental illness (ID: WO/2021/111116). GM has received consulting fees from Boehringer Ingelheim and speaker fees from Johnson & Johnson.

ETHICS APPROVAL AND CONSENT TO PARTICIPATE

All methods were performed in accordance with the relevant guidelines and regulations. Ethical approval for this study was obtained from the London/Surrey Research Ethics Committee (17/LO/1130). All participants provided written informed consent before participation.

ADDITIONAL INFORMATION

Supplementary information The online version contains supplementary material available at <https://doi.org/10.1038/s41380-025-03204-9>.

Correspondence and requests for materials should be addressed to Paulina B. Lukow.

Reprints and permission information is available at <http://www.nature.com/reprints>

Publisher's note Springer Nature remains neutral with regard to jurisdictional claims in published maps and institutional affiliations.



Open Access This article is licensed under a Creative Commons Attribution 4.0 International License, which permits use, sharing,

adaptation, distribution and reproduction in any medium or format, as long as you give appropriate credit to the original author(s) and the source, provide a link to the Creative Commons licence, and indicate if changes were made. The images or other third party material in this article are included in the article's Creative Commons licence, unless indicated otherwise in a credit line to the material. If material is not included in the article's Creative Commons licence and your intended use is not permitted by statutory regulation or exceeds the permitted use, you will need to obtain permission directly from the copyright holder. To view a copy of this licence, visit <http://creativecommons.org/licenses/by/4.0/>.

© The Author(s) 2025